ELSEVIER

Ceramics International 30 (2004) 1787–1791

CERAMICS INTERNATIONAL

www.elsevier.com/locate/ceramint

Comparison of hydroxyapatite ceramics and hydroxyapatite/borosilicate glass composites prepared by slip casting

Yifei Hu, Xigeng Miao*

School of Materials Engineering, Nanyang Technological University, Nanyang Avenue, Singapore 639798, Singapore

Received 12 November 2003; received in revised form 28 November 2003; accepted 22 December 2003

Available online 6 May 2004

Abstract

Borosilicate glass powder with a softening point of 821 °C was prepared by crushing Pyrex® borosilicate glass fragments. Hydroxyapatite (HA) ceramics and HA/borosilicate glass (50 wt.%) composites were prepared by slip casting. The influence of borosilicate glass on the densification and phase change of hydroxyapatite was studied over sintering temperatures from 500 to 1200 °C. It was found that the borosilicate glass inhibited the decomposition of HA phase and enhanced the densification of the composites. When the sintering temperature was higher than 1100 °C, the glass liquid flowed away from the sample surface and was trapped inside the sample, leading to a structure of a relatively strong and dense HA/glass core and a bioactive and porous HA surface layer.

Keywords: B. Composite; Hydroxyapatite; Borosilicate glass

1. Introduction

Hydroxyapatite (HA, $Ca_{10}(PO_4)_6(OH)_2$) is the main mineral constituent of teeth and bone. It exhibits no cytoxic effects and shows excellent biocompatibility with hard tissues and with skin and muscle tissues. Furthermore, HA ceramics can bond to bone. All these facts make HA the most appropriate ceramic material for bone replacement. However, the mechanical properties of pure HA are poor. For example the fracture toughness (K_{Ic}) of pure HA is not more than 1 MPa $m^{1/2}$, while the fracture toughness of human bone is up to 12 MPa $m^{1/2}$ [1]. Currently, pure HA ceramics cannot be used as load-bearing implants, but are often used in the form of coatings. Unfortunately, the interfacial strength between a substrate and the HA coating is normally very low, which leads to the failure of the implant [2]. One way to improve the HA ceramics and coatings is the addition of a glass as a second phase. In fact, bioglass-reinforced HA ceramics have been recently developed and characterized in terms of mechanical properties [3,4]. The composites exhibit better mechanical properties and bioactivity than HA ceramics, both as coatings and as bulk materials [5,6]. Another way of improving the interfacial bonding strength is the use of plasma-spray deposition [7]. However, this coating method has limitations when it is used for the coating of porous ceramic materials. To coat the internal surfaces of an open porous ceramic material, dip coating with a sol or a slurry (or slip) is an appropriate method due to its ability to coat the internal pore wall surfaces [11].

Recently, the authors have produced uniform and graded porous zirconia ceramics [8]. Since zirconia is bioinert, it is important to have a bioactive coating. In order to study the possibility of coating the porous zirconia with a HA/glass layer by dip-coating method, the present study, as the initial stage, was to prepare HA/glass composite bulk materials by slip casting, as slip casting is similar to dip coating in many aspects and is simpler than dip coating in terms of processing. In this study, borosilicate glass was added into HA matrix to enhance the mechanical properties of HA. Borosilicate glass was used because it is bioinert, easily obtained, and much cheaper than bioactive glass. In most glass-modified hydroxyapatite ceramics, only up to 5 wt.% glass was used in order to enhance bioactivity or mechanical properties [3–5,9,10]. However, for the purpose of coating, a higher content of glass was needed [11]. Thus, in this study, 50 wt.% glass was selected and added into HA matrix. HA/glass composites were then prepared by slip casting with the HA/glass slurry. The microstructural development of the composites was studied over different sintering tempera-

* Corresponding author. Tel.: +65-67904260; fax: +65-67909081.
E-mail address: asxgmiao@ntu.edu.sg (X. Miao).

0272-8842/$30.00
doi:10.1016/j.ceramint.2003.12.119

tures. The study would provide some insights on HA/glass composite as a coating material for porous zirconia.

2. Experimental procedure

The two main starting materials were commercial HA powder and borosilicate glass powder prepared in-house. The commercial HA powder (Riedel-de Haë®) had an average particle size of 0.11 μm. The borosilicate glass powder was obtained by crushing Pyrex® borosilicate glass fragments into glass frits, followed by planetary ball milling and attrition milling. The particle size of the borosilicate glass powder was 0.50 μm, as measured by a particle size analyzer (Brookhaven BI-XDC). The borosilicate glass had the following standard composition: 81 wt.% of SiO_2, 4 wt.% of Na_2O, 0.5 wt.% of K_2O, 13 wt.% of B_2O_3, and 2 wt.% of Al_2O_3. The softening point of the glass was 821 °C, which was measured by a differential thermal analyzer (NETZSCH DSC 404). The density of the glass was 2.23 g/cm^3, as determined by a pycnometer (AccuPyc 1330 V2.01). To prepare HA/glass slurry, a mixture of 50 wt.% HA and 50 wt.% glass was ball milled with distilled water. The solids loading of the HA/glass slurry was 45 wt.% and the content of the dispersant (Darvan® C, 25 wt.% ammonium polymethacrylate (NH_4-PMAA) solution) was 0.8 wt.%. The mixed slurry was cast into a gypsum mold and dried in air for 3 days. The green cast bodies were then sintered at 500–1200 °C in air. For comparison, pure HA samples were also prepared in the same way by slip casting.

The prepared samples were characterized by several techniques. The bulk densities of the pure HA ceramics and the HA/glass composites sintered at different temperatures and subjected to grinding and rough polishing, were obtained by measuring the weights and volumes of the samples. The relative densities of the samples were then calculated using the following expressions:

$$\text{Relative density of HA} = \frac{\text{Bulk density of HA}}{\text{Theoretical density of HA}}\% \quad (1)$$

$$\text{Relative density of composite} = \frac{\text{Bulk density of composite}}{\text{Theoretical density of composite}}\% \quad (2)$$

where the theoretical density of HA is 3.16 g/cm^3 and the theoretical density of HA/glass composite is 2.62 g/cm^3, as calculated according to the law of mixture. For the microstructural characterization, scanning electron microscopy (SEM) was used to observe the surface morphologies of both polished cross-sections and as-sintered surfaces. X-ray diffraction (Lab XRD-6000 Shimadzu) was also performed on the as sintered surfaces to identify the phases present in the samples. Finally, for mechanical characterization, hardness was measured by a Vickers hardness tester (HSV-20 Shimadzu) on the as sintered surfaces.

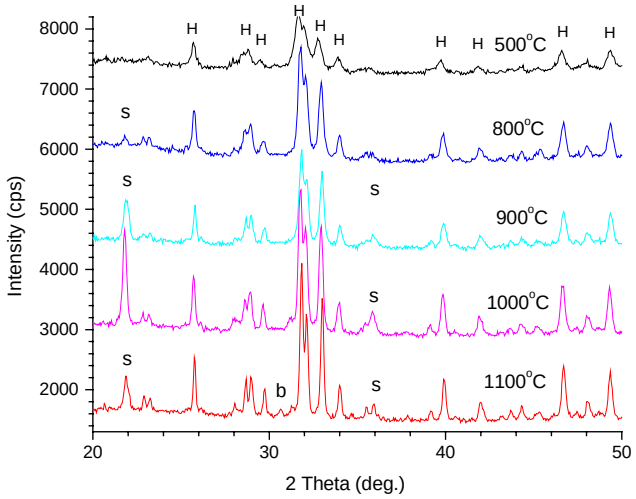

Fig. 1. X-ray diffraction patterns for HA/glass composites sintered at from 500 to 1100 °C (s: SiO_2, b: β-TCP, H: HA).

3. Results and discussion

3.1. Phase development in the HA/glass composites

The X-ray diffraction patterns of the HA/glass composites sintered at different temperatures are shown in Fig. 1. It can be seen that silica (tridymite, JCPDS #140260) peaks appeared at 800 °C and the intensity of the peaks increased with the sintering temperature and reached a maximum at 1000 °C. However, the intensity of the silica peaks decreased at 1100 °C. This can be explained by the crystallization of the borosilicate glass component. Below 800 °C, the glass powder was amorphous, but above 800 °C, the glass was subjected to crystallization. The silica peak intensity decreased above 1000 °C, due to melting of the glass at high temperatures. The molten glass could not stay on the surface of the composite due to the gravity and the capillary forces from the HA matrix. Thus, the surface of the composite became depleted in SiO_2 and the molten glass trapped inside the composite would later become solidified during cooling.

From Fig. 1, one can see that a small amount of beta-tricalcium phosphate (β-TCP) was found at 1100 °C in the HA/glass composite. As a comparison, Fig. 2 shows the XRD patterns of pure HA ceramics sintered at 800, 900, and 1000 °C, respectively. The formation of β-TCP was observed at the sintering temperature of 1000 °C. Thus, it can be seen that the glass addition did not harm the stability of the HA phase; on the contrary, the glass slightly stabilized the HA phase. The stabilization of HA phase by the glass could be understood by referring to the following discussion.

The thermal decomposition of HA into alpha-tricalcium phosphate (α-TCP) and β-TCP has been widely reported. Two steps are associated with the thermal decomposition: dehydroxylation and decomposition. The dehydroxylation of HA to oxyhydroxyapatite proceeds by a fully reversible

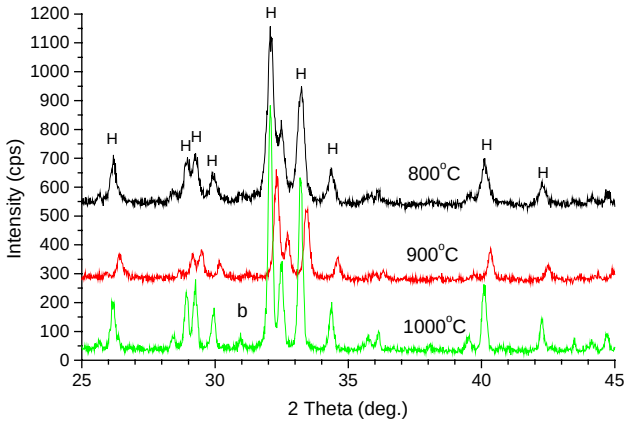

Fig. 2. X-ray diffraction patterns for HA sintered at from 800 to 1000 °C (H: HA, b: β-TCP).

reaction at temperatures from about 850 to 900 °C [12]:

$$Ca_{10}(PO_4)_6(OH)_2 \rightarrow Ca_{10}(PO_4)_6(OH)_{2-2x}O_x + xH_2O_{gas} \quad (3)$$

On the other hand, the decomposition of HA to TCP and tetracalcium phosphate occurs at temperatures higher than 900 °C by the following reaction:

$$Ca_{10}(PO_4)_6(OH)_2 \rightarrow 2Ca_3(PO_4)_2 + Ca_4P_2O_9 + H_2O_{gas} \quad (4)$$

Since both dehydroxylation and decomposition reactions involve water vapor as a product, one can tailor the rates for these reactions by controlling the sintering atmosphere especially the water vapor partial pressure. One can also suppress the release of water vapor by encapsulating the HA grains or particles. The fact that adding borosilicate glass could slightly inhibit the decomposition of HA can be explained by the encapsulation of HA with the glass. Since the glass began to soften above 800 °C, the glass phase dispersed in the HA matrix would embrace the HA particles. Thus, less surface area of the HA particles was exposed to air, resulting in the slow down of the decomposition. However, when the sintering temperature was higher than 1000 °C, the fluidity of the glass increased, and the glass failed to stay on the surface of the HA/glass composite due to gravity and capillary forces. Thus, the porous HA surface layer was exposed to air and the decomposition of HA phase occurred.

The borosilicate glass used in this study was a non-phosphate-based glass and it had the function of stabilizing the HA phase. This was in contrast to the results obtained from the addition of a phosphate-based glass. Rey et al. [13] and Raemdonck et al. [14] reported that the imbalance in the Ca/P ratio of HA due to the addition of a phosphate-based glass could lead to the formation of β-TCP below 1200 °C and α-TCP above 1200 °C [15].

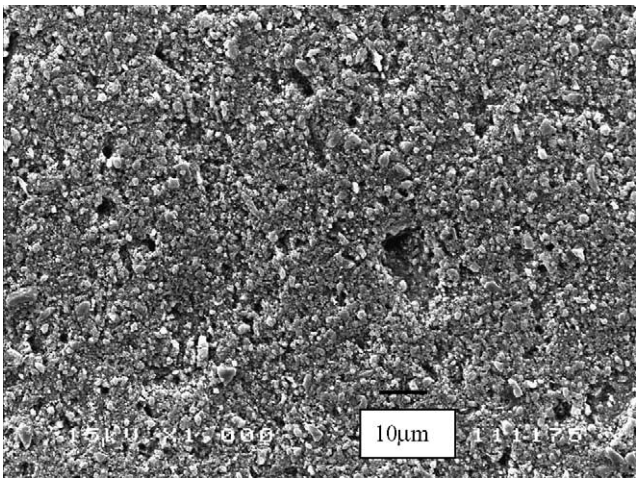

Fig. 3. SEM micrograph of a cross-section of the HA/glass composite sintered at 800 °C for 1 h.

3.2. Densification of the HA/glass composites

The SEM micrographs of the cross-sections of the HA/glass composites are shown in Figs. 3–5. Since the softening point of the borosilicate glass was 821 °C, one can see from the SEM micrographs that the morphology changed dramatically with the sintering temperature from 800 to 900 °C. Specifically, after the HA/glass composite was sintered at 800 °C, the borosilicate glass particles were dispersed uniformly in the HA matrix just as in the original green compact of the HA/glass powder mixture. Above the softening point, the glass began to soften and then became a viscous liquid that was able to hold the HA particles together. The higher the sintering temperature, the less viscous the glass became. At 1200 °C, the liquid phase sintering mechanism prevailed in the composite, resulting in very dense interior of the composite.

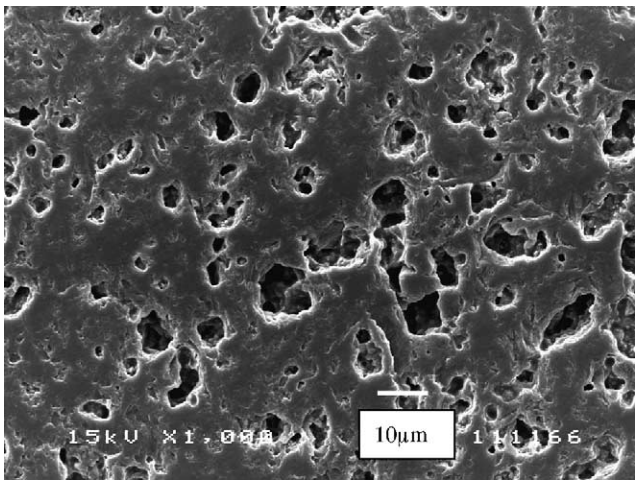

Fig. 4. SEM micrograph of a cross-section of the HA/glass composite sintered at 900 °C for 1 h.

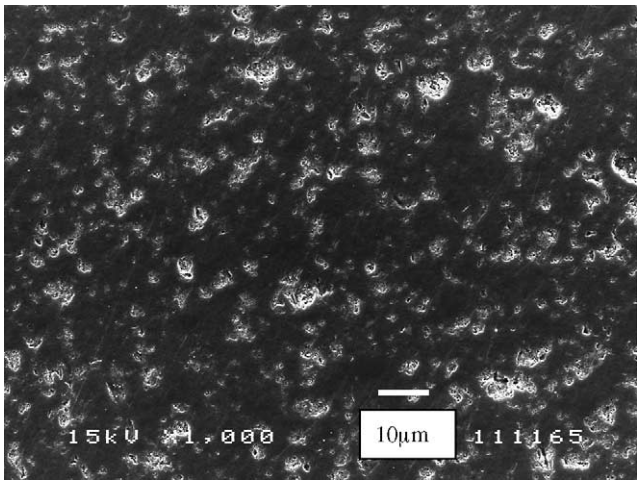

Fig. 5. SEM micrograph of a cross-section of the HA/glass composite sintered at 1200 °C for 1 h.

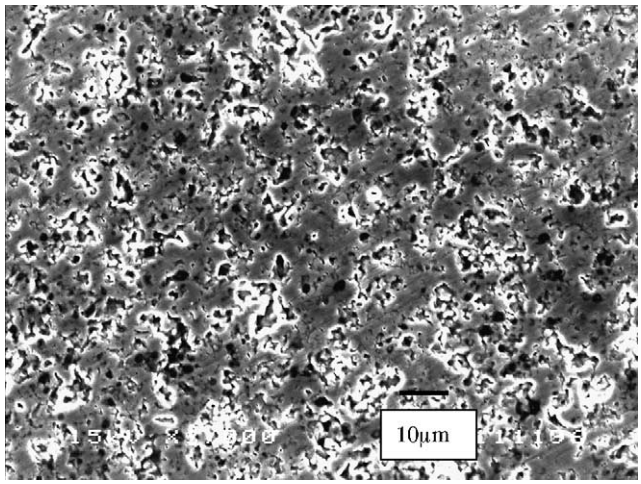

Fig. 7. SEM micrograph of a cross-section of the pure HA sample sintered at 1200 °C for 1 h.

Fig. 6 is a micrograph of the as-sintered surface of the HA/glass composite sintered at 1200 °C. Only porous HA surface layer that contained no glass was observed. This was because the sintering temperature was too high for the borosilicate glass to stay on the surface of the HA/glass composite. After melting, the glass liquid tended to be trapped inside the HA matrix in the interior of the sample. The porous HA surface layer could provide beneficial effect as it would increase the bioactivity of the composite on the surface. In other words, although high glass (bioinert) content was used in the study, the surface bioactivity could still be maintained due to the enrichment of the HA phase on the surface. Fig. 7 is a micrograph of the cross-section of the pure HA sample. Compared to the HA/glass composite sintered at the same temperature (Fig. 5), the pure HA sample was more porous than the composite. The porous microstructure resulted from the incomplete densification of the HA particles. Thus, the glass powder had acted as a sintering aid in the HA/glass composite. Finally, the densities of the HA/glass composites and the pure HA ceramics are shown in Fig. 8. It is obvious that the addition of the borosilicate glass improved the densification of HA ceramics.

3.3. Vickers hardness

The results of Vickers hardness tests are shown in Fig. 9. The increase of hardness with sintering temperature for pure HA samples was attributed to the higher degree of densification, while the variation of hardness with sintering temperature for the HA/glass composites was because of the addition of borosilicate glass. At the sintering temperature of 800 °C, there was little hardness difference between the HA/glass composites and the pure HA samples. However, once the glass passed its softening point (i.e. from 900 to 1000 °C), the hardness increased abruptly due to the much increased densification of the samples. However, further increase in the sintering temperature resulted in the

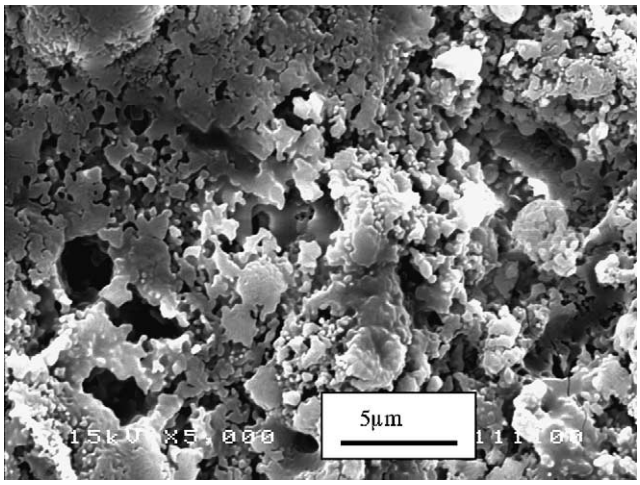

Fig. 6. SEM micrograph of an as-sintered surface of the HA/glass composite sintered at 1200 °C for 1 h.

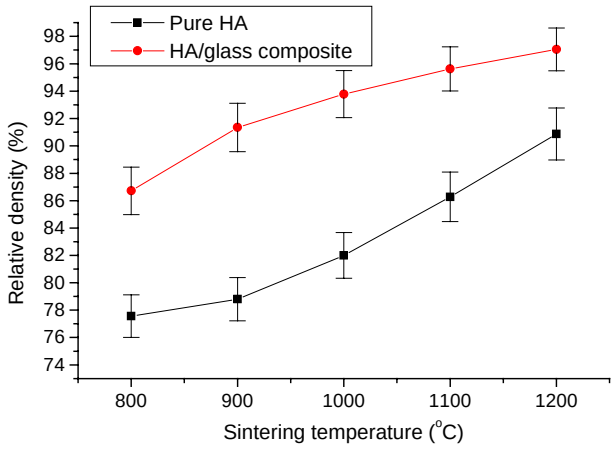

Fig. 8. Relative density of pure HA ceramics and HA/glass composites sintered at different temperatures.

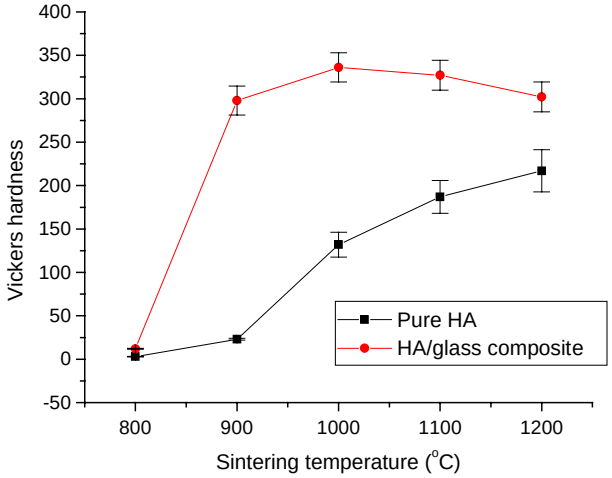

Fig. 9. Vickers hardness of pure HA ceramics and HA/glass composites sintered at different temperatures.

decrease of the hardness value. This can be understood by the way of the hardness measurement; the indentation was done on the as sintered surfaces. As mentioned before, the top surfaces became porous when the sintering temperature caused the flow of glass liquid. The relatively soft HA porous layers would nevertheless have desirable bioactivity.

4. Conclusions

Borosilicate glass powder remained amorphous below 800 °C, but crystallized to form SiO_2 tridymite (JCPDS #140260) between 800 and 1000 °C, and became glass liquid above 1100 °C. Pure HA ceramics only achieved 90% relative density after sintering at 1200 °C for 1 h. When 50 wt.% borosilicate glass was added into hydroxyapatite matrix, the densification and the phase development of the HA/glass composites were modified compared to the pure HA ceramics. The borosilicate glass was able to facilitate the densification process due to the viscous glass flow. The borosilicate glass also was able to stabilize the HA phase against thermal decomposition due to the encapsulation of HA phase by the glass phase. The improved densification resulted in increased hardness of the HA/glass composites. Interestingly, when the sintering temperature was higher than 1100 °C, the glass liquid flowed away from the sample surface and was trapped inside the sample, leading to a structure of a relatively strong and dense HA/glass core and a bioactive and porous HA surface layer.

Acknowledgements

The authors would like to acknowledge the financial support from the Nanyang Technological University in Singapore (AcRF RG26/01).

References

[1] W. Suchanek, M. Yoshimura, Processing and properties of hydroxyapatite-based biomaterials for use as hard tissue replacement implants, J. Mater. Res. 13 (1) (1998) 94–117.
[2] J.M. Romez-Vega, E. Saiz, A.P. Tomsia, Glass–hydroxyapatite coatings on titanium-based implants, in: L. George, et al. (Eds.), Bioceramics: Materials and Applications III, American Ceramic Society, 2000, pp. 15–21.
[3] M.A. Lopes, F.J. Monteiro, J.D. Santos, A.P. Serro, B. Sara-mago, Hydrophobicity, surface tensions, and zeta potential measurements of glass-reinforced hydroxyapatite composites, J. Biomed. Mater. Res. 45 (1999) 370–375.
[4] J.D. Santos, P.L. Silva, J.C. Knowles, S. Talal, F.J. Monteiro, Reinforcement of hydroxyapatite by adding P_2O_5–CaO glasses with Na_2O, K_2O and MgO, J. Mater. Sci.: Mater. Med. 7 (1996) 187–189.
[5] M.A. Lopes, J.C. Knowles, L. Kuru, J.D. Santos, F.J. Monteiro, I. Olsen, Flow cytometry for assessing biocompatibility, J. Biomed. Mater. Res. 41 (1998) 649–656.
[6] A.C. Queiroz, J.D. Santos, F.J. Monteiro, M.H. Prado da Silva, Dissolution studies of hydroxyapatite and glass-reinforced hydroxyapatite ceramics, Mater. Charact. 50 (2–3) (2003) 197–202.
[7] V. Deram, C. Minichiello, R.-N. Vannier, A. Le Maguer, L. Pawlowski, D. Murano, Microstructural characterizations of plasma sprayed hydroxyapatite coatings, Surf. Coat. Technol. 166 (2003) 153–159.
[8] X. Miao, Y. Hu, J. Liu, B. Tio, P. Cheang, K.A. Khor, Highly interconnected and functionally graded porous bioceramics, Key Eng. Mater. 240–242 (2003) 595–598.
[9] M.A. Lopes, J.D. Santos, F.J. Monteiro, J.C. Knowles, Glass-reinforced hydroxyapatite: a comprehensive study of the effect of glass composition on the crystallography of the composite, J. Biomed. Mater. Res. 39 (1998) 244–251.
[10] G. Georgious, J.C. Knowles, Glass reinforced hydroxyapatite for hard tissue surgery—part 1: Mechanical properties, Biomaterials 22 (2001) 2811–2815.
[11] G. Jiang, D. Shi, Coating of hydroxyapatite on highly porous Al_2O_3 substrate for bone substitutes, J. Biomed. Mater. Res. 43 (1998) 77–81.
[12] T.P. Hoepfer, E.D. Case, Physical characteristics of sintered hydroxyapatite, in: L. George (Ed.), Bioceramics: Materials and Applications III, American Ceramic Society, 2000, pp. 53–67.
[13] C. Rey, M. Freche, M. Heughebaert, M. Vignoles, Apatite chemistry in biomaterial preparation, shaping and biological behaviour, in: W. Bonfield, G.W. Hastings, K.E. Tanner (Eds.), Bioceramics, vol. 4, Butterworth-Heinemann, London, 1991, pp. 57–64.
[14] W. Raemdonck, P. Ducheyne, P. Meester, Calcium phosphate ceramics, in: P. Ducheyne, G.W. Hastings (Eds.), Metal and Ceramic Materials, CRC Press, Boca Raton, FL, 1984, pp. 143–175.
[15] J.D. Santos, J.C. Knowles, R.L. Reis, F.J. Monteiro, G.W. Hastings, Microstructural characterization of glass-reinforced hydroxyapatite composites, Biomaterials 15 (1994) 5–10.